ELSEVIER

Journal of Electroanalytical Chemistry 467 (1999) 230–237

JOURNAL OF ELECTROANALYTICAL CHEMISTRY

Influence of the electric potential on the structure of pyridine adlayers on Au(111) terraces from in-situ scanning tunnelling microscopy imaging☆

G. Andreasen, M.E. Vela, R.C. Salvarezza, A.J. Arvia *

Instituto de Investigaciones Fisicoquímicas Teóricas y Aplicadas (INIFTA, Conicet-Unlp-Cic), Facultad de Ciencias Exactas, Universidad Nacional de La Plata, Sucursal 4, Casilla de Correo 16, (1900) La Plata, Argentina

Received 14 July 1998; received in revised form 4 January 1999; accepted 15 January 1999

Abstract

The adsorption and desorption of pyridine (Py) adlayers prepared on Au(111) terraces were studied by in-situ scanning tunnelling microscopy (STM) and conventional voltammetry using an aqueous 0.1 M $HClO_4 + 10^{-4}$ M Py solution at 298 K. The applied potential covered the range 0.15 V $< E <$ 1.2 V (vs. SHE), i.e. potentials above and below E_{pzc}, the potential of zero charge of Au(111). In the range $E_{pzc} < E <$ 0.96 V, hexagonal (4×4) ordered domains corresponding to Py molecules adsorbed vertically on the Au(111) surface coexist with disordered adlayer domains, but for $E < E_{pzc}$, the ordered adlayer structure disappears leaving uncovered Au(111) domains. Similarly, for $E >$ 0.96 V, the (4×4) adlayer lattice is removed completely leading to a bare Au(111) surface. By stepping E backwards to a value in the range $E_{pzc} < E <$ 0.96 V, the readsorption of Py takes place and the (4×4) adlayer domains are recovered in a few minutes. STM data offer the possibility of discussing anion adsorption and the early electroformation stages of the OH-containing adlayer on Au(111) terraces.

Keywords: Scanning tunnelling microscopy; Electric potential; Pyridine adlayers; Au(111) terraces

1. Introduction

Among adsorption processes involving organic molecules on well-characterized metal surfaces, the adsorption of pyridine (Py) on Au single crystals has been considered as a model system [1]. The adsorption isotherm of Py from neutral aqueous 0.1 M $NaClO_4$ on Au(111) at 298 K has been related to two different adlayer configurations, depending on whether the applied potential (E) was more positive or negative than the potential of zero charge of Au(111), $E_{pzc} \cong 0.5$ V versus SHE at 298 K [2]. When $E < E_{pzc}$, adsorbed Py molecules display the parallel π-bonded orientation reaching a maximum surface concentration (Γ_m) close to $\Gamma_m = 1.4 \times 10^{-10}$ mol cm^{-2}. The corresponding Gibbs energy of adsorption is $\Delta G^0_{ad} < 30$ kJ mol^{-1}, as expected for physisorbed Py molecules [3]. Otherwise, when $E \geq E_{pzc}$, an increase to $\Gamma_m = 6.7 \times 10^{-10}$ mol cm^{-2} and $\Delta G^0_{ad} = 38$ kJ mol^{-1} has been reported [1]. This change in the values of Γ_m has been interpreted as a reorientation of adsorbed Py molecules from a parallel to a vertically N-bonded configuration, and the value $\Delta G^0_{ad} = 38$ kJ mol^{-1} has been ascribed to a weakly chemisorbed state of Py on Au(111) [1]. Similar results have been reported for Py adsorption on polycrystalline Au from aqueous 0.1 M $HClO_4$, at 298 K [4]. In this case, the adsorption of Py on the positively charged Au surface is probably preceded by the deprotonation of pyridonium ions, and it involves the value $\Delta G^0_{ad} = 22 \pm 2$ kJ mol^{-1} [4].

Recent in-situ scanning tunnelling microscopy (STM) data [5] have shown that the adsorption of Py on Au(111) terraces from aqueous 0.1 M $HClO_4 + 10^{-3}$ M

☆ Dedicated to Jean Clavilier on the occasion of his retirement from LEI CNRS and in recognition of his contribution to Interfacial Electrochemistry.

* Corresponding author. Fax: +54-221-4254642.

E-mail address: ajarvia@inifta.unlp.edu.ar (A.J. Arvia)

0022-0728/99/$ - see front matter
PII: S0022-0728(99)00035-2

Py, at 298 K, for $E_{pzc} < E < 0.6$ V versus SHE results in ordered (4×4) domains of vertically adsorbed Py molecules coexisting with disordered domains in which no molecular resolution could be obtained. Correspondingly, the Py adlayer structure becomes more complex than previously thought, and therefore, for $E > E_{pzc}$, the value $\Gamma_m = 6.7 \times 10^{-10}$ mol cm^{-2} obtained from electroadsorption measurements has to be considered as an average coverage value resulting from coexisting ordered and disordered domains. It was also observed that by stepping the potential from $E_{pzc} < E < 0.6$ V to $E < E_{pzc}$ the gradual disappearance of ordered domains and, simultaneously, the partial desorption of Py molecules occurs, resulting in dilute Py adlayer domains and uncovered Au(111) terraces. It was also concluded that the potential step-induced Py adlayer rearrangement behaves as a structurally reversible process with a duration of several minutes.

In contrast to the above information, little is known about the influence of the electrode potential and Py concentration on the structure of Py adlayers, particularly at potentials close to that where the early stages of the Au oxide monolayer electroformation on Au(111) takes place, i.e. for $E > 0.96$ V versus SHE.

This paper deals with the adsorption–desorption of Py adlayers on Au(111) terraces covering the range $0.15 \text{ V} < E < 1.2$ V versus SHE, at 298 K, from aqueous 0.1 M $HClO_4 + 10^{-4}$ M Py, that is a Py concentration one order of magnitude lower than that used in [5]. These processes were followed by combining in-situ STM imaging and electrochemical measurements. For $E_{pzc} < E < 0.96$ V, it was found that the hexagonal (4×4) Py adlayer domains corresponding to vertically adsorbed Py molecules coexist with disordered domains as already reported for 10^{-3} M Py [5]. Likewise, for $E < E_{pzc}$, ordered adlayer domains tend to disappear leading to a disordered Py adlayer and uncovered Au(111) domains. On the other hand, for $E \cong 0.96$ V, the (4×4) Py adlayer lattice is removed completely by electrooxidation leaving bare Au(111). Stepping the potential from either $E < E_{pzc}$ or $E > 0.96$ V to a value in the range $E_{pzc} < E < 0.96$ V, the readsorption of Py on Au(111) brings the (4×4) Py lattice back in a few minutes. Several aspects of surface electrochemistry of Au(111) in aqueous $HClO_4$ in the potential range $E_{pzc} < E = 0.96$ V, such as the adsorption of ClO_4^- ions, the electrodesorption of Py, and the early stages of OH-containing adlayer electroformation are discussed throughout the conclusions derived from STM imaging data.

2. Experimental

Experiments consisted of voltammetry measurements and in-situ STM imaging at the nm level, at 298 K, in a N_2 atmosphere. Three-electrode electrochemical cells consisting of the working electrode, a Pt counter-electrode and a Pd | H reference electrode were used. Each working electrode (hereafter referred to as the Au substrate) was a 250-nm thick Au layer evaporated onto Robax glass (AF Berliner Glass KG, Germany) with a 2-nm thick Cr undercoating for better adhesion to the glass surface. Before each experiment, the Au substrate was annealed under a H_2 flame to obtain flat Au terraces [5]. Two solutions were used, aqueous 0.1 M $HClO_4$ (for blanks) and aqueous 0.1 M $HClO_4 + 10^{-4}$ M Py. They were prepared from the highest purity chemicals (Merck) and Milli-Q* water.

Voltammetry was run in a conventional electrochemical cell employing a PAR 273 instrument. The absence of impurities at the electrochemical interface was checked through voltammetry. Any distortion in the well-known shape of the Au(111) voltammogram in aqueous 0.1 M $HClO_4$ could be detected in these runs.

In-situ STM images were taken using Nanoscope III electrochemical STM equipment (Digital Instruments, Santa Barbara CA). In this case, the electrochemical cell was mounted inside a glass bell under a steady N_2 flux to avoid oxygen interference. Commercial Pt–Ir tips (Digital Instruments, Santa Barbara CA) covered by Apiezon wax to reduce the faradaic current at the tip | electrolyte interface were used. In addition, the tip potential (E_{tip}) was adjusted in the range $0.3 \le E_{tip} \le 0.6$ V, i.e. in the double layer potential region, as concluded from voltammetric data for the Pt–Ir tip in the working solution. Typical tunnelling conditions were in the ranges $0.06 \text{ V} \le E_{bias} \le 1.0$ V and $500 \text{ pA} \le I \le 20$ nA.

3. Results

3.1. Voltammetry data

The voltammogram of the Au substrate immersed in aqueous 0.1 M $HClO_4 + 10^{-4}$ M Py run at 0.1 V s^{-1} in the range $0.15 \text{ V} \le E \le 1.70$ V (Fig. 1(a)) shows the double layer region and the current peaks related to the electroformation/electroreduction of the Au oxide monolayer that has been already described for the blank [5]. The presence of Py in the solution produces an anodic current contribution starting from 1.1 V upwards, a delay in the electroformation of the Au oxide monolayer, a negative shift of the threshold electroreduction potential of the Au oxide monolayer, and makes the double layer region slightly broader than that of Au(111) in aqueous 0.1 M $HClO_4$ [5]. A more detailed inspection of the voltammogram cover-

ing the range 0.15–1.15 V (Fig. 1(b)) shows a small anodic current peak (AI) at $E = 0.40$ V, a well-defined anodic peak (AII) located at $E = 0.73$ V, and a third peak (AIII) at $E = 0.96$V. The reverse potential scan shows that the pairs of peaks CI/AI, CII/AII, and CIII/AIII behave as conjugated peaks. The pair of peaks AI/CI that has been observed in plain aqueous $HClO_4$ solution has been related to ClO_4^- ion adsorption [6–8]. The height of these peaks decreases by holding the potential at the potential of peak AII (Fig. 1(b)). The pair of peaks AII/CII has been related to Py adsorption/desorption [5]. Otherwise, the pair of peaks AIII/CIII has been assigned to Py electrooxidation/electroreduction [9]. The height of this pair of peaks increases by holding the potential at the potential of peak AII. The differences in the anodic/cathodic charge density ratio for the pair of peaks AIII/CIII suggests that only a negligible amount of products from the electrooxidation of Py can be electroreduced in the reverse potential scan. Finally, the anodic and cathodic current contributions observed at 1.15 V are related to the early stages of AuOH monolayer formation [6].

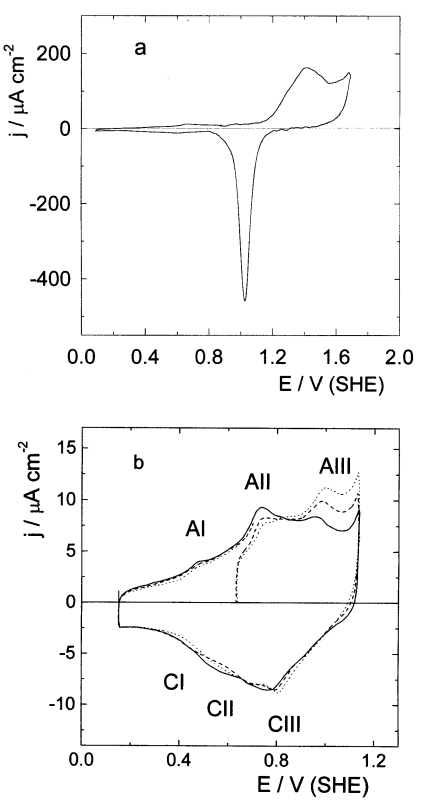

Fig. 1. Apparent current density (j) vs. potential (E) voltammograms for the Au substrate in aqueous 0.1 M $HClO_4 + 10^{-4}$ M pyridine run at 0.10 V s^{-1}. $T = 298$ K. (a) Potential range 0.15–1.75 V. (b) Double-layer potential region (solid trace). Dotted and dashed traces indicate voltammograms initiated at 0.64 V after a holding time $t = 20$ min (dashed trace) and $t = 75$ min (dotted trace).

3.2. STM imaging data

In-situ high-resolution STM images of Py adlayers on Au(111) terraces in aqueous 0.1 M $HClO_4 + 10^{-4}$ M Py (Fig. 2) demonstrate that the structure of these adlayers depends on the applied potential. Thus, at $E = 0.7$ V (Fig. 2(a)), i.e. $E > E_{pzc} = 0.525$ V [2], images show ordered domains with the (4×4) hexagonal lattice involving the nearest neighbor distance $d = 0.38$ nm, as has been found for Py adsorption on Au(111) from aqueous 0.1 M $HClO_4 + 10^{-3}$ M Py, in the same potential range [5]. The (4×4) hexagonal lattice can be imaged over the entire range of operation conditions namely, $0.06\ V \leq E_{bias} \leq 1.0$ V and $500\ pA \leq I_{tip} \leq 20$ nA. However, lowering E_{bias} to 0.02 V at $I_{tip} = 20$ nA, the (4×4) lattice is replaced by the hexagonal pattern with $d = 0.29$ nm of unreconstructed (1×1) Au(111). Then, as the tunnelling resistance decreases, the tip-induced removal of the Py adlayer leads to a bare Au(111) surface.

The (4×4) adlayer lattice has been assigned to Py molecules chemisorbed perpendicularly on Au(111) through the N atom [5], in agreement with conclusions derived previously from Py electroadsorption on Au(111) for $E > E_{pzc}$ [1,3]. Schemes of the (4×4) Py adlayer lattice showing the location of N atoms imaged by STM, and the possible arrangement of Py molecules are depicted in Figs. 2(b and c), respectively. Recently, a similar molecular arrangement has been proposed for the adsorption of uracil molecules on Au(111) [10]. However, the size of vertically adsorbed Py molecules to be arranged in the (4×4) lattice is 0.50×0.29 nm^2 (Fig. 2(c)). The 0.29 nm molecular thickness value is certainly close to the theoretical value estimated for the π-orbitals, but the 0.50 nm molecular width value is smaller than the value of 0.53 nm estimated for the aromatic ring in the free molecule. This difference would indicate that a certain distortion of the Py molecule takes place during adsorption on Au(111). This assumption is supported by X-ray data for crystallized Py as in this case the molecule width is reduced to 0.5 nm [11]. Furthermore, from SERS studies it is also known that the adsorption of Py occurs through the interaction of the metal atom with the N lone-pair electrons of Py that extends through the π-electron system, producing significant changes in the electronic structure of the molecule [12]

It is often also found that STM images of the (4×4) Py adlayer (Fig. 2(d)) exhibit a hexagonal array of black spots with $d = 1.0$ nm that have been assigned to vacancies in the adlayer. The Fourier spectra of these images show that the black spot lattice is rotated 30° with respect to the (4x4) Py adlayer lattice (Fig. 2(e)). As has been concluded from adsorption energy consideration [13] these vacancies correspond to sites where Py molecules are adsorbed atop Au atoms.

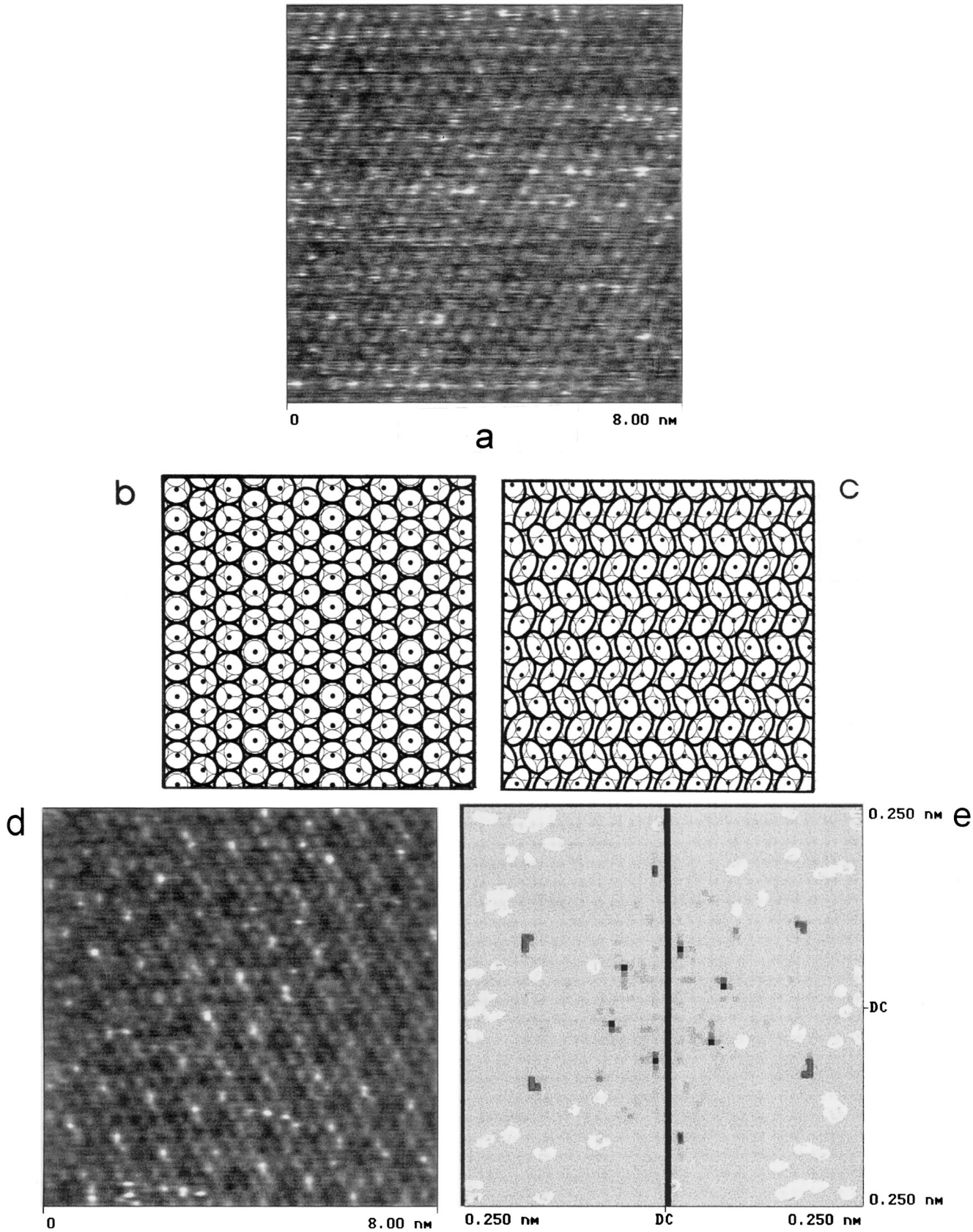

Fig. 2. (a) In-situ STM image (8×8 nm^2, raw data) at $E = 0.70$ V. Molecular resolution of the (4×4) Py adlayer can be observed. (b) Scheme showing the position of the N atom in the (4×4) Py overlayer on Au(111). Large circles denote the N atom of the Py molecule and the small circles correspond to Au atoms. Black dots indicate adsorption sites at the Au(111) substrate. (c) A scheme of a possible arrangement of Py molecules in the (4×4) adlayer. (d) In-situ STM image (8×8 nm^2, raw data) at $E = 0.70$ V. Black holes corresponding to Py vacant sites in the (4×4) Py adlayer can be observed. (e) Fourier spectrum of the image shown in (d). The outer hexagonal pattern corresponds to the (4×4) Py adlayer, and the inner 30° rotated hexagonal pattern corresponds to vacancies in the Py adlayer.

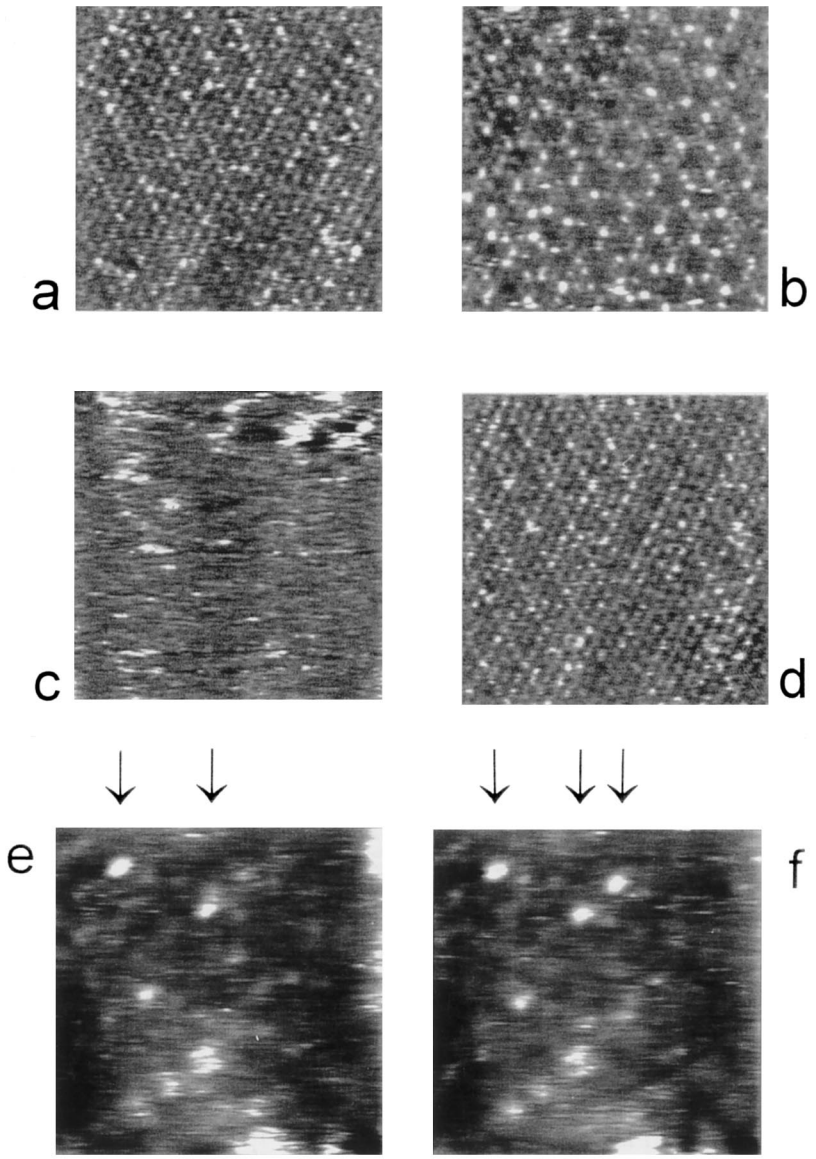

Fig. 3. In-situ STM (8×8 nm^2) images at different values of E. (a) $E = 0.70$ V. The (4×4) Py adlayer is observed. (b) After stepping from $E = 0.70$ to 0.25 V. A large density of vacancies can be seen. (c) After stepping from $E = 0.25$ to 0.15 V. A blurred image is obtained. (d) After stepping the potential back from $E = 0.15$ to 0.70 V. After 3 min the (4×4) Py layer reappears. (e, f) Sequential STM images (10×10 nm^2) at $E = 0.15$ V. The arrows indicate mobile bright spots of a size compatible with the cross section of Py molecules parallel to the Au(111) surface.

As E is decreased stepwise from 0.70 to 0.25 V (Fig. 3(a)), that is a potential lower than E_{pzc}, the black spot pattern is enhanced and around these spots the disorder at the Py adlayer increases (Fig. 3(b)). This image exhibits a more disordered distribution of Py adsorbate (bright spots). As E is further decreased stepwise from 0.25 to 0.15 V, a blurred STM image (Fig. 3(c)) that reflects the dilute and mobile nature of the physisorbed Py adlayer is obtained. For $E < E_{pzc}$ a weak Py(π-orbital)–Au(111) interaction has been concluded previously from electrochemical measurements [1,3]. Finally, when E is stepped back to $E = 0.7$ V the (4×4) Py lattice is recovered after a few minutes (Fig. 3(d)). Occasionally, mobile bright spots of a size compatible with that of the cross section of a Py molecule lying parallel to the Au(111) surface can be imaged (Figs. 3(e and f)).

On the other hand, when E is changed stepwise from 0.70 V (Fig. 4(a)) to $E > 0.96$ V, the (4×4) Py lattice (Fig. 4(a) and its cross section) disappears rapidly. Despite the fact that the STM images are somewhat blurred, it is possible to conclude that most of the surface exhibits the hexagonal (1×1) unreconstructed Au(111) lattice with $d = 0.29$ nm (Fig. 4(b)). The images shown in Figs. 4(a and b) confirm that there is no rotation of the (4×4) Py lattice with respect to the Au(111) lattice, as has been already suggested [5]. Otherwise, STM images following the change of E from

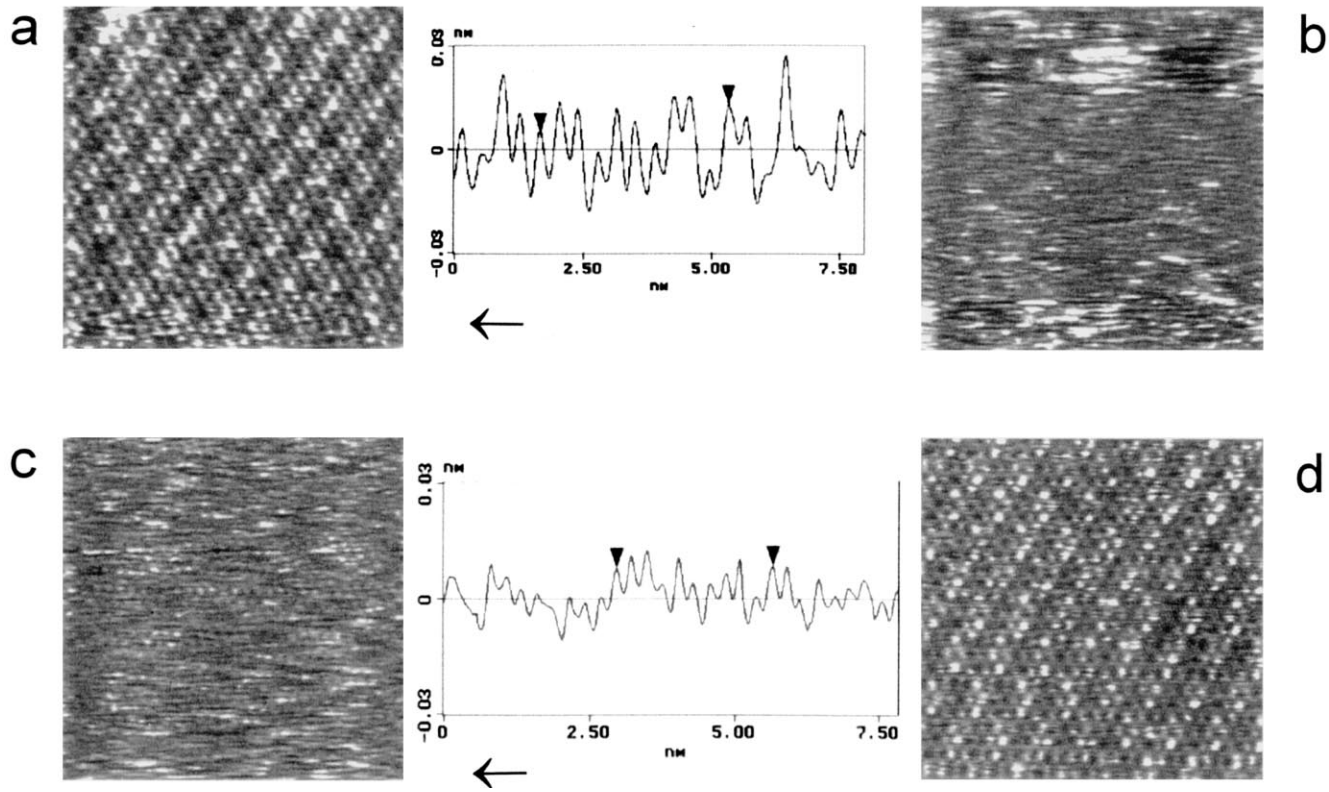

Fig. 4. In-situ STM (8×8 nm^2) images at different values of E. (a) $E = 0.70$ V. The (4×4) Py adlayer is observed. The corresponding cross section is included. (b) After stepping from $E = 0.70$ to 0.96 V. A blurred image with domains exhibiting the (1×1) Au(111) lattice can be seen. (c) STM image taken immediately after stepping from $E = 0.96$ to 0.70 V. The (1×1) Au(111) lattice continues being observed. The corresponding cross section is included. The difference in corrugation ($z = 0.01$ nm) and nearest neighbour distance ($d = 0.29$ nm) as compared to $z = 0.02$ nm and $d = 0.38$ nm of Py adlayer shown in (a) can be noticed. (d) The STM image taken 3 min after image (c), showing the reappearance of the (4×4) Py adlayer.

0.96 to 0.70 V, that is a potential more negative than the threshold potential for the electroadsorption of OH on Au(111) from a H_2O molecule, show that the bare Au(111) lattice with the Py-containing solution remains practically unchanged for a few minutes (Fig. 4(c) and cross section) before a net adsorption of Py is observed. Finally, the Au(111) surface becomes fully covered by the 4×4 Py lattice for $t = 5$ min (Fig. 4(d)).

4. Discussion

4.1. Preliminary considerations

STM images of Au(111) in Py-containing aqueous $HClO_4$ provide new information about the behavior of Py adlayers on Au(111) terraces under different applied potential conditions. In fact, results show that an ordered Py adlayer is formed in the range $E_{pzc} < E < 0.96$ V, whereas for $E > 0.96$ V the Py adlayer is electrodesorbed completely from the Au substrate, a process that is related to voltammetric peak AIII. The appearance of peak AIII is consistent with previously reported information about the electrooxidation of Py on noble metals in neutral media [9].

The fact that only the (4×4) Py adlayer and the (1×1) unreconstructed Au(111) lattices can be observed in the potential range $E_{pzc} < E < 0.96$ V turns out to be of particular interest in discussing further details on the behaviour of the Au(111) surface within this range of potential where several possible interactions including the formation of certain adlayer structures have been postulated on the basis of electrochemical measurements [1–3]. Therefore, an attempt is made to establish greater coherence between electrochemical and STM imaging data in relation to ordered adlayer structures, the electroadsorption and electrodesorption of the Py adlayer, and their implications for the earlier stages of O-containing adlayer formation on Au(111).

4.2. Ordered adlayers resulting from STM imaging and electroadsorption processes

Blank experiments showed that there is a voltammetric charge related to Au(111)-perchlorate ion interaction in the range $E_{pzc} < E < 0.96$ V, as has already been reported [6,7]. The corresponding voltammetric charge has been related to almost fully discharged ClO_4^- ions

forming a dilute adlayer with a low degree of surface coverage ($\theta \approx 0.2$, for aqueous 0.1 M $HClO_4$). The symmetry of the Au(111) surface lattice would have a strong influence on the specific adsorption of ClO_4^- ions because of the matching of the tetrahedral ion with the trigonal symmetry of the unreconstructed Au(111) plane [6,7]. However, from STM imaging there is no evidence for the formation of an ordered ClO_4^- ion adlayer in the range $E_{pzc} < E < 0.96$ V in plain aqueous $HClO_4$ as only the (1×1) Au(111) lattice can be observed [5]. Therefore, the tip-substrate interaction appears to be sufficiently strong to remove weakly adsorbed ClO_4^- ions from Au(111). This interpretation is supported by the fact that an ordered sulphate ion adlayer structure on Au(111) has been observed by STM due to the stronger substrate–sulphate ion interaction [14–16]. It has been proposed that ClO_4^- ion behaves as a non-specifically adsorbed anion on unreconstructed (1×1) Au(111) [17].

On the other hand, STM images confirm the appearance of (4×4) Py adlayer domains on Au(111) in dilute Py-containing aqueous $HClO_4$ in the range $E_{pzc} < E <$ 0.96 V, i.e. the potential range where the adsorbed Py molecule is vertically N-bonded to Au(111). For Py electroadsorption on Au(111) values for the maximum surface concentration of adsorbate, $\Gamma_m = 6.7 \times 10^{-10}$ mol cm^{-2}, and for polycrystalline Au the electroadsoportion valence, $\gamma = 0.6$, have been reported [18]. It is clear that in the range $E_{pzc} < E < 0.96$ V, the adsorption of Py on Au(111) from 10^{-4} M Py in aqueous $HClO_4$ is relatively slow and it lasts a few minutes. In this case, the Py–Au(111) interaction energy appears to be higher than the Au(111)–ClO_4^- ion interaction energy at the electrical double layer. This is consistent with the progressive decrease in the influence of ClO_4^- ions on the capacitance versus E plots of the Au (polycrystalline) | Py-containing aqueous $HClO_4$ interface as the concentration of Py in the solution is increased [4].

On the other hand when the potential is stepped from a value of E compatible with the (4×4) lattice to $E < E_{pzc}$, the partial desorption and a rearrangement of the Py adlayer can be observed. In this case, STM images (Fig. 3) indicate that the desorption process involves the formation of vacancies starting from the desorption of Py molecules located at the lowest adsorption energy sites (atop sites). In fact, when E is stepped to 0.25 V a greater density of vacancies and an increasing disorder in the remaining adlayer result. Py adlayer desorption and rearrangement processes also take place in the order of few minutes. Finally, when $E < 0.15$ V, blurred STM images compatible with a dilute and mobile Py adlayer are obtained. Bright spots observed occasionally at $E < 0.15$ V correspond to Py molecules lying parallel to the electrode surface, as was already concluded from electrochemical data [1–3].

4.3. Electrooxidation of the Py adlayer and the early stages of OH-electroadsorption

The (4×4) Py adlayer disappears very fast from the Au(111) surface at $E = 0.96$ V, i.e. a potential that coincides with the potential of voltammetric peak AIII (Fig. 1(b)). In this potential range Py electrodesorption would be expected to occur simultaneously with the electroadsorption of OH from the discharge of water molecules. However, no clearcut structural evidence of adsorbed OH species in the potential range preceding the formation of the O-containing monolayer on Au(111) [6] could be found from STM imaging. Possible explanations for these results are the low degree of surface coverage by OH species at the early stages of O-containing monolayer formation and the relatively short half-life time of these species, which is of the order of 1 ms, as concluded from triangularly modulated triangular potential sweep voltammetry [19]. This short half-life time indicates that the initially formed OH surface species is weakly bound to Au assisting the formation of a mobile dilute OH adlayer. Then, the random displacement of the OH adlayer on the Au(111) surface should be considered as either of the same order as or greater than the scanning rate of the STM tip. This situation can explain the somewhat lower resolution of blurred STM images resulting for the Au(111) lattice at $E = 0.96$ V (Fig. 4) as compared to those obtained at lower values of E [5]. Another possible explanation is that the OH adlayer adopts the same (1×1) lattice as that of Au(111). However, current peaks associated with the early stages of AuOH adlayer electroformation and electroreduction are clearly observed at $E > 1.15$ V, i.e. at potentials more positive than those where the Py layer is electro-oxidized. Then, it is reasonable to conclude that the degree of surface coverage of Au(111) by OH species is sufficiently low to be captured by STM, leaving only the possibility of imaging bare domains of Au(111).

Finally, no measurable change in the surface corrugation could be observed at $E = 0.96$ V. In fact, the increase in surface corrugation of the Au substrate has been observed when its anodization in the aqueous acid solution was extended up to the Au oxide monolayer potential range [20,21]. Furthermore, it has been reported that the resolution of (1×1) Au(111) is prevented at $E = 1.22$ V, i.e. a potential very close to the onset of oxidation of Au(111) [21].

5. Conclusions

(i) In the range $E_{pcz} < E < 0.96$ V ordered (4×4) domains of vertically adsorbed molecules are present on Au(111) terraces in 0.1 M $HClO_4 + 10^{-4}$ M Py.

(ii) After Py adlayer electrochemical removal at $E = 0.96$ V, a fast process taking place at the potential range of peak AIII, STM imaging shows only the (1×1) lattice of the Au(111) surface.

(iii) Py readsorption is a relatively slow process that lasts a few minutes and yields backwards the (4×4) Py adlayer lattice.

(iv) At $E < E_{pcz}$ Py partially desorbs slowly from the Au(111) surface decreasing surface coverage and leading to a dilute and mobile adlayer of molecules lying parallel to the substrate surface.

Acknowledgements

This work was supported financially by the Consejo Nacional de Investigaciones Científicas y Técnicas (CONICET) (PIP 014/97), Agencia Nacional de Promoción Científica y Tecnológica (PICT 97-01993) and the Comisión de Investigaciones Científicas de la Provincia de Buenos Aires (CIC).

References

[1] J. Lipkowski, L. Stolberg, in: P. Lipkowski, P. Ross, (Eds.), Adsorption of Molecules at Metal Electrodes, VCH, New York, 1992, p. 171, and references therein.
[2] L. Stolberg, S. Morin, J. Lipkowski, D.E. Irish, J. Electroanal. Chem. 307 (1991) 241.
[3] J. Lipkowski, L. Stolberg, D.F. Yang, B. Pettinger, S. Mirwald, F. Henglein, D.M. Kolb, Electrochim. Acta 39 (1994) 1045.
[4] M.M. Gómez, M.P. García, J. San Fabián, L. Vázquez, R.C. Salvarezza, A.J. Arvia, Langmuir 13 (1997) 1317.
[5] G. Andreasen, M.E. Vela, R.C. Salvarezza, A.J. Arvia, Langmuir 13 (1997) 6814.
[6] H. Angerstein-Kozlowska, B.E. Conway, A. Hamelin, L. Stoicoviciu, Electrochim. Acta 31 (1986) 1051.
[7] H. Angerstein-Kozlowska, B.E. Conway, K Tellefsen, B. Barnett, Electrochim. Acta 34 (1989) 1045.
[8] H. Hamelin, in: A. Gewirth, H. Siegenthaler (Eds.), Nanoscale Probes of the Solid | Liquid Interface, Kluwer, Dordrecht, 1995, p. 285.
[9] L. Stolberg, J. Lipkowski, D.E. Irish, J. Electroanal. Chem. 296 (1990) 171.
[10] Th. Dretschkow, A.S. Dakkouri, Th. Wandlowski, Langmuir 13 (1997) 2843.
[11] D. Mootz, H.G. Wussow, J. Chem. Phys. 75 (1981) 1517.
[12] S. Efrima, in: Modern Aspects of Electrochemistry, vol. 16, Plenum Press, New York, 1985, Chap. 4, p. 253.
[13] J.A. Rodriguez, Surf. Sci. 226 (1990) 101.
[14] J. Edens, X. Gao, M.J. Weaver, J. Electroanal. Chem. 375 (1994) 357.
[15] Th. Dretschkow, Th. Wandlowski, Ber. Bunsenges. Phys. Chem. 101 (1998) 749.
[16] Z. Shi, J. Lipkowski, M. Gamboa, P. Zeleny, A. Wieckowski, J. Electroanal. Chem. 366 (1994) 317.
[17] P. Mrozek, Y.-E. Sung, A. Wieckowski, Surf. Sci. 335 (1995) 44.
[18] L. Stolberg, J. Richer, J. Lipkowski, D.E. Irish, J. Electroanal. Chem. 207 (1986) 213.
[19] C.M. Ferro, A.J. Calandra, A.J. Arvia, J. Electroanal. Chem. 59 (1975) 239.
[20] C.M. Vitus, A. Davenport, J. Electrochem. Soc. 141 (1994) 1291.
[21] H. Honbo, S. Sugawara, K. Itaya, Anal. Chem. 62 (1990) 272.